ANNALES
UNIVERSITATIS MARIAE CURIE-SKŁODOWSKA
LUBLIN - POLONIA
VOL. L/LI SECTIO AAA 1995/1996

Institute of Physics, M. Curie-Skłodowska University,
20-031 Lublin, pl. M. Curie-Skłodowskiej 1, Poland

PIOTR ROZMEJ, ROBERT ARVIEU*

Wave Packet Dynamics — New Collapse and Revival Structures

Dynamika pakietów falowych — nowe struktury kollapsu i odbudowy

6672

1. INTRODUCTION

Studying the dynamics of wave packets in simple quantum systems like molecules, hydrogen atom, billiards and cavities receives recently rapidly growing attention. The aim of these studies is to distinguish the genuine quantum properties from the classical ones with the particular emphasis on the time dependent aspects. Development of experimental techniques (short, intense laser pulses) allows for creation and analysis of wave packet motion in hydrogen and hydrogenoid atoms. In such systems electrons can be excited to a coherent mixture of many Rydberg states that move almost classically for many Kepler periods [1–2]. Long range time evolution of such wave packets exhibits spreading and revivals according to the universal scenario described in [3–5]. These quantum effects arise from nonequidistant spectrum of energy levels in the Coulomb field.

* Institut des Sciences Nucléaires, F 38026 Grenoble–Cedex, France

2. SPIN–ORBIT PENDULUM

In a series of papers [6–10] we have described an essentially new phenomenon in nonrelativistic quantum mechanics, spin–orbit pendulum. Here we give only a brief description of main results contained there.

It was shown in a simple model, that the spin–orbit interaction can produce a new dynamical structures of collapses and revivals. The model discussed consists of the spherical oscillator Hamiltonian with a spin–orbit interaction whose coupling constant is κ,

$$H = H_{HO} + V_{ls} = H_{HO} + \kappa\,(\vec{l}\cdot\vec{s})\ . \tag{1}$$

The system is integrable, motion is periodic with two different frequencies. One of them is the classical frequency corresponding to the Kepler period, the other one is the frequency of the spin–orbit motion, directly related to the spin–orbit splitting of single particle energy levels (and determined by the value of coupling constant κ). The wave packet, initially well localized, and representing a definite spin polarization in the orbit's plane, splits during the evolution into two subpackets. In the reference frame moving as classical particle (i.e. according to HO part of the Hamiltonian) the subpackets move in the opposite directions. This motion is accompanied by the appropriate adjustments of the spin field in subpackets. They gain the opposite polarization, different from the initial one, in a way analogous to the Stern–Gerlach effect. The loss and regain of the overlap of the subpackets, with respective changes of phases, cause the periodic transfer of a fraction of average angular momentum between the spin and the orbital subspaces. Due to periodicity these changes are reversed during the second part of the T_{ls} period. The spin–orbit pendulum phenomenon is displayed for the case $\overline{n} = 8$ in Figure 1, the corresponding time dependence of the

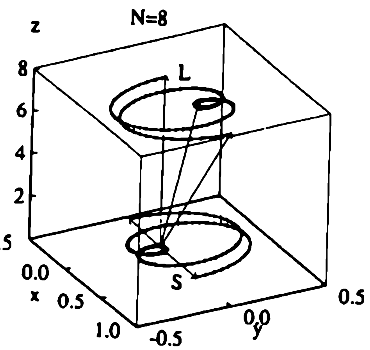

Fig. 1. Motion of $\langle\vec{s}\rangle$ and $\langle\vec{l}\rangle$ during $t \in [0, T_{ls}/2]$ illustrating oscillations and exchange of angular momenta (*spin–orbit pendulum*) for $\overline{n} = 8$. Symbols show the equidistant time steps $T_{ls}/500$

Ruch $\langle\vec{s}\rangle$ i $\langle\vec{l}\rangle$ w przedziale czasu $t \in [0, T_{ls}/2]$ ilustrujący oscylacje i wymianę momentu pędu (wahadło spinowo–orbitalne) dla $\overline{n} = 8$. Symbolami oznaczono kolejne punkty z krokiem czasowym $T_{ls}/500$

quantity representing the purity of the wave packet in spin subspace $\mathrm{Tr}\rho^2$ is shown in Figure 2. In Figure 3 we present the density probability of the wave packet $\Psi^\dagger\Psi$ and the spin density field $\Psi^\dagger\vec{s}\,\Psi$ for two instants of time, $t = 0$ and $t = \frac{1}{4}T_{ls}$.

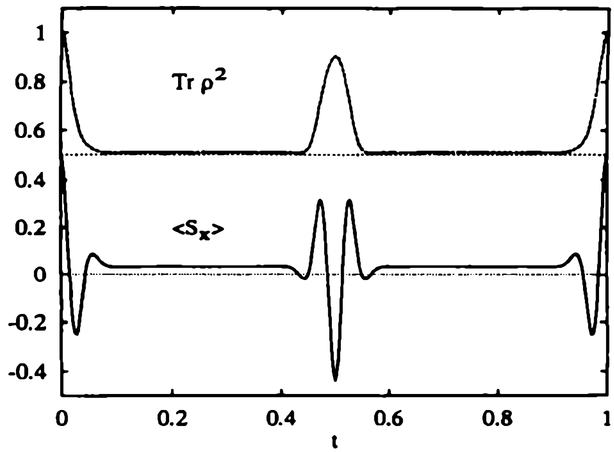

Fig. 2. Expectation value of the spin component $\langle s_x\rangle$ and purity of the wave function $\mathrm{Tr}\rho^2$ as functions of time for $\overline{n} = 8$ case. Time in units of T_{ls}
Wartość średnia składowej spinu $\langle s_x\rangle$ i czystość stanu $\mathrm{Tr}\rho^2$ jako funkcje czasu dla przypadku $\overline{n} = 8$. Jednostki czasu w T_{ls}

We expect that these new dynamical structures in wave packet motion should also be present if instead of HO potential one chooses the Coulomb field. Till now nobody has considered spin–orbit coupling in atomic systems because in the context of wave packet dynamics this coupling is negligibly small. In other words time scale for the spin–orbit motion is in standard atomic cases much too long to allow for any observations. In [7] we have shown that our theory, for the case of circular orbits, can be directly applied (in perturbation approach) to the case of the Coulomb field. Then we could calculate the characteristic times for the collapse and revival structures. These times are: T_{clas} — the period of the classical motion corresponding to one revolution of the packet along the orbit, T_{rev} — the revival time, the shortest time for approximate full revival of the wave packet (it determines also the times of fractional revivals), and T_{ls} — the period of spin–orbit motion. Our aim is to find conditions under which the ratio T_{ls}/T_{rev} is as small as possible. Only then there are chances for experimental observation of predicted dynamical behaviour caused by spin–orbit interaction. Let Z stands for the nuclear charge and N for the mean value of the principal

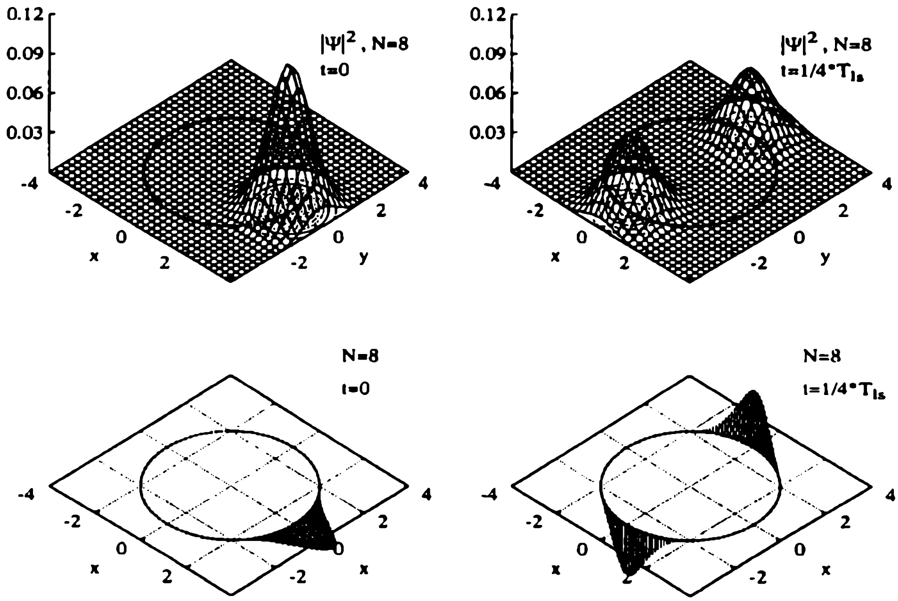

Fig. 3. Illustration of the motion of the wave packet with $\overline{n} = 8$ at time instants $t = 0$ and $t = \frac{1}{4}T_{ls}$. $|\Psi(t)|^2$ is shownas the function of coordinates on the plane of the classical orbit (marked with the thick circle) — top, and spin density field $\Psi^{\dagger}(t)\vec{s}\,\Psi(t)$ (only along the orbit) — bottom. The motion is presented in reference frame moving according to HO Hamiltonian (i.e. as classical particle)

Ilustracja ruchu pakietowego o $\overline{n} = 8$ w chwilach czasowych $t = 0$ oraz $t = \frac{1}{4}T_{ls}$. Rycina przedstawia $|\Psi(t)|^2$ jako funkcje współrzędnych na płaszczyźnie orbity klasycznej (zaznaczonej grubym okręgiem) — część górna, oraz pole gęstości spinowej $\Psi^{\dagger}(t)\vec{s}\,\Psi(t)$ (tylko wzdłuż orbity) — część dolna. Ruch jest przedstawiony w układzie odniesienia poruszającym się zgodnie z klasyczną cząstką

quantum number in the wave packet. Then the three characteristic times scale with Z and N as follows: $T_{\rm clas} \propto N^3/Z^2$, $T_{\rm rev} \propto N^4/Z^2$ and $T_{ls} \propto N^5/(\alpha^2 Z^4)$. It is then obvious that to minimize the ratio $T_{ls}/T_{\rm rev}$ one has to choose Z as big as possible. On the other hand $\overline{n}$ (in standard atomic experiments of the order of 10^2 [1–2]) must be simultaneously substantially reduced. All past theoretical predictions [3–5] of the universal scenario of collapses and revivals based on analytical formulas which become exact in the limit of high $\overline{n}$. As we are interested in low $\overline{n}$ limit (N of the order of 10) we have to reject the approximate formulas valid for high $\overline{n}$ limit and to make our calculations exactly (numerically).

3. CIRCULAR WAVE PACKETS IN COULOMB FIELD

Let us construct a circular wave packet in a standard way [3–5] as a superposition of circular–orbit eigenfunctions with Gaussian weights, centered at a principal quantum number $\overline{n}$. The wave function describing this wave packet is at $t = 0$

$$|\Psi(t=0)\rangle = \frac{1}{(2\pi\sigma^2)^{1/4}} \sum_{n=1}^{\infty} \exp\left[-\left(\frac{n-\overline{n}}{2\sigma}\right)^2\right] \Psi_{n,n-1,n-1}(r,\theta,\phi)\,, \quad (2)$$

where $\overline{n}$ and σ are the mean and the standard deviation of the Gaussian distribution, respectively.

$$\Psi_{n,n-1,n-1}(r,\theta,\phi) = A_n\, r^{(n-1)}\, e^{-r/n}\, \sin^{(n-1)}\theta\, e^{i(n-1)\phi} \quad (3)$$

is an aligned standard hydrogenic eigenfunction with $l = m = n-1$, where A_n is a normalization constant. During the evolution each term gains a phase factor $e^{it/2n^2}$ and the wave packet at time t is given by

$$|\Psi(t)\rangle = \frac{1}{(2\pi\sigma^2)^{1/4}} \sum_{n=1}^{\infty} \exp\left[-\left(\frac{n-\overline{n}}{2\sigma}\right)^2\right] \Psi_{n,n-1,n-1}(r,\theta,\phi)\, e^{it/2n^2}\,. \quad (4)$$

Time evolution of such circular wave packets was considered by many authors [3–5, 11], mainly in the context of comparison of the quantum evolution to the classical one. Therefore all authors considered wave packets with large $\overline{n}$. In this limit there exists a hierarchy of collapses, fractional and full revivals and also longer term structures sometimes referred to as superrevivals [11]. The most general discussion is given by Peres [5]. Let us rewrite (4) in the simplified form: $|\Psi(\vec{r},t)\rangle = \sum_n c_n u_n(\vec{r})\, e^{it/2n^2}$. Obviously $\int u_n^* u_s d\vec{r} = \delta_{ns}$ and $\sum_n |c_n|^2 = 1$. This sum converges, therefore a finite number of c_n makes it arbitrarily close to 1 and is sufficient to represent Ψ with arbitrary accuracy. Then any Ψ is arbitrarily close to a periodic function of time [12]. Let L be the common multiple of all n for which c_n are not neglected. Then Ψ has a period $T_{\text{clas}}L^2$. The recurrence with this period is exact, but if many levels contribute to the sum (4) the required time is enormously long. However nearly exact recurrences occur considerably earlier. The hierarchy of recurrence times is the following: $T_1 = (\overline{n}/3 + \frac{1}{2})T_{\text{clas}}$, $T_2 = (\overline{n}^2/4 + \frac{1}{2})T_{\text{clas}}$, $T_3 = (\overline{n}^3/5 + \frac{1}{2})T_{\text{clas}}$, $T_4 = (\overline{n}^4/6 + \frac{1}{2})T_{\text{clas}}$, etc. [5].

The convenient measure of the degree of recurrences is the recurrence probability (also referred to as autocorrelation function), where $w_n = |c_n|^2$,

$$P(t) = |\langle\Psi(0)|\Psi(t)\rangle|^2 = \sum_n w_n\, e^{it/2n^2}\,. \quad (5)$$

Below we present the results of numerical calculations for the evolution of the wave packet (4) with parameters suitable for inclusion of the spin–orbit interaction. They are the following: $\overline{n} = 12$, $\sigma = 1$ and the summation in the wave packet is taken from $n_1 = 2$ to $n_2 = 22$.

In Figures 4–5 we have presented the recurrence probability as a function of time (time units equal $T_{\rm clas}$) for this wave packet, and in Figure 6 the probability density $\Psi^{\dagger}(t)\Psi(t)$ in the plane of classical orbit for six different times. The evolution of the wave packet with low quantum numbers exhibits less complicated structures than that with high quantum numbers. In particular in the short time scale only the lowest order fractional revivals can be observed. In our case $T_{\rm rev} = T_1 = 4.5$ and this recurrence is well seen in Figure 4.

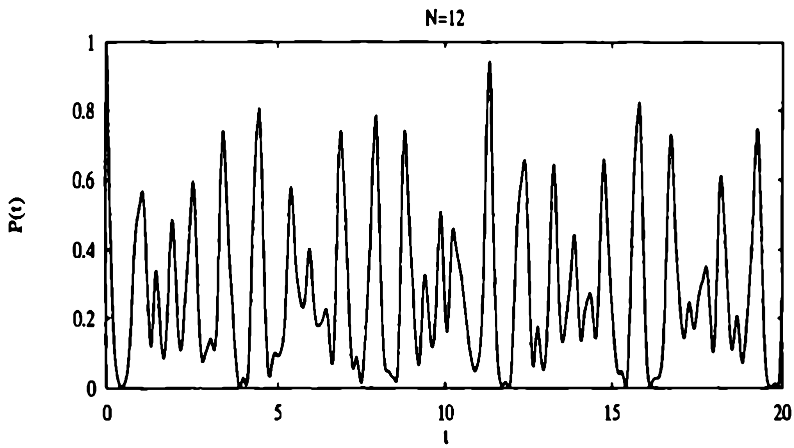

Fig. 4. The recurrence probability (5) for the wave packet with $\overline{n} = 12$ as a function of time (in units of $T_{\rm clas}$) for $t \in [0, 20]$. Note frequency doubling at $t \approx 2, 7, 10\ldots$ The most prominent recurrence for this time range achieve the value 0.9444 for $t = 11.3444$
Prawdopodobieństwo powtórzenia (5) pakietu falowego o $\overline{n} = 12$ jako funkcji czasu (w jednostkach $T_{\rm clas}$) dla $t \in [0, 20]$. Widoczne jest podwajanie się częstości w chwilach $t \approx 2, 7, 10\ldots$. Największe prawdopodobieństwo powtórzenia osiąga w tym przedziale czasowym wartość 0,9444 dla $t = 11{,}3444$

Around half of this time the frequency doubling corresponding to fractional revival of $\frac{1}{2}$ order is clearly seen. It corresponds to the division of the wave packet into two comparable subpackets moving on the opposite ends of the orbit's diameter, which is clearly seen from Figure 6 at $t = 2$. It is worth mentioning that the values of $P(t)$ which are very close to zero do not mean that wave packet is spread almost uniformly over the orbit. It means that the packet is well localized, but far from the initial position and therefore

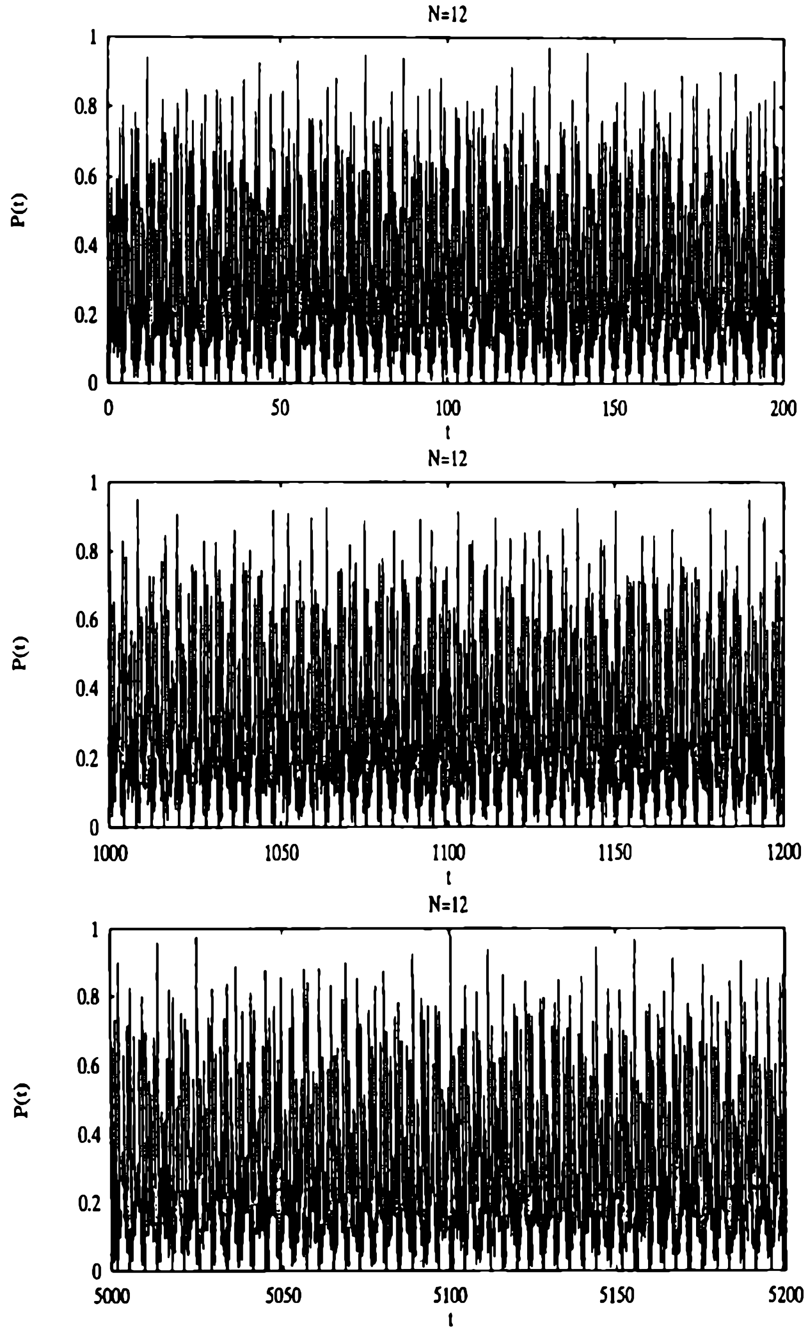

Fig. 5. The same as in Fig. 4 but for time ranges [0, 200] (top), [1000, 1200] (middle) and [5000, 5200] (bottom). The best recurrence occurs for $t = 5100.4$ and achieves the value 0.9828 but there are many other strong recurrences, too

To samo, co na rycinie 4, ale dla przedziałów czasu [0, 200] (góra), [1000, 1200] (środek) i [5000, 5200] (dół). Najlepsze powtórzenie zachodzi dla $t = 5100{,}4$ i osiąga wartość 0,9828, ale jest wiele innych, również bardzo dobrych

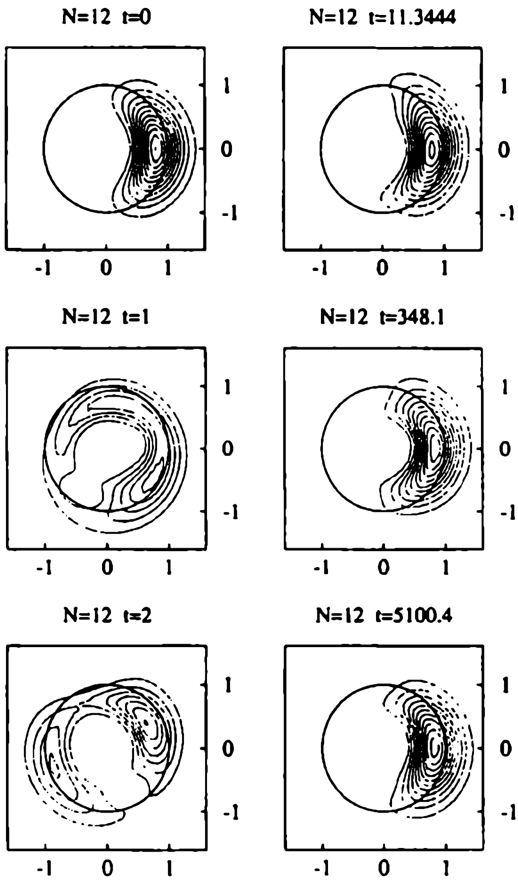

Fig. 6. Contour plots of probability density $\Psi^\dagger(t)\Psi(t)$ as function of coordinates (in units of the classical radius) on the plane of classical orbit (thick circle). The time unit is $T_{\rm clas}$. Note spreading of the wave packet at $t = 1$, fractional revival of the order $\frac{1}{2}$ at $t = 2$, and almost perfect revivals at times $t = 11.3444$, 348.1 and 5100.4

Wykres konturowy gęstości prawdopodobieństwa $\Psi^\dagger(t)\Psi(t)$ jako funkcji współrzędnych na płaszczyźnie klasycznej orbity (w jednostkach jej promienia, orbita zaznaczona grubym okręgiem). Jednostką czasu jest $T_{\rm clas}$. Widoczne jest rozpływanie się pakietu dla $t = 1$, ułamkowa odbudowa rzędu 1/2 w chwili $t = 2$ i prawie doskonała odbudowa pakietu falowego w chwilach $t = 11,3444$, 348,1 oraz 5100,4 the overlap is very small. For almost uniformly spread wave packet one obtains the overlap 0.2–0.3 for our case, which as it is seen from Figure 5 is the most frequent value (the dark area). In Figure 6 the form of the wave packet (4) is displayed for six different times. At $t = 0$ the packet is well localized. Due to low quantum numbers it spreads very rapidly, and already after one classical revolution is spread over the entire orbit. At $t = 2$ two subpackets almost separated are formed which corresponds to fractional revival of $\frac{1}{2}$ order. In the right column of Figure 6 the wave packets at 3 times in which the recurrence probability takes large values are presented. The upper case corresponds to $t = 11.3444$ for which $P(t) = 0.9444$ (the best recurrence in Figure 4). The middle case corresponds to $t = 348.1$ where $P(t) = 0.94$ and the bottom case is for $t = 5100.4$, where $P(t) = 0.9828$. As is clearly seen from the figure, the revivals are almost perfect, practically they are very good already when $P(t) \geqslant 0.8$. From Figure 5 we see that there are plenty of such revivals during the evolution.

4. CONCLUSIONS

We have demonstrated that wave packets with low quantum numbers exhibit strong revival structures during their evolution. If we choose the physical system as a hydrogen–like ion composed of uranium nuclei ($Z = 92$) and one electron it is in principle possible to construct a wave packet with relatively low principal quantum numbers. Such systems are already available for experiments in GSI storage ring, and first experiments to excite and analyse the electronic states have been done [13]. For $\overline{n} = 12$ and $Z = 92$ the ratio $T_{ls}/T_{\rm clas} \approx 320$. This means that the effects of spin–orbit coupling should manifest themselves already in the time scale of 160 classical revolutions (half of T_{ls} period) and should be noticed during the wave packet lifetime. We predict then the following behaviour: the recurrence probability shown in Figure 5 should be modulated by a function similar to that shown in Figure 3 ($\mathrm{Tr}\rho^2$) when plotted in the same units. The expected behaviour is plotted in the Figure 7.

Although the above estimations of relative time scales look rather promising, the absolute time scales add a questionmark to chances for experimental observations of predicted dynamical structures. The increase of Z and the choice of low $\overline{n}$ numbers changes relevant energy scale (and the corresponding time scale) to ranges which actually may be not available in physical laboratories. In present experiments [1, 2] picosecond lasers are used for systems with Z close to one to excite states in range $\overline{n} \approx 50$ with

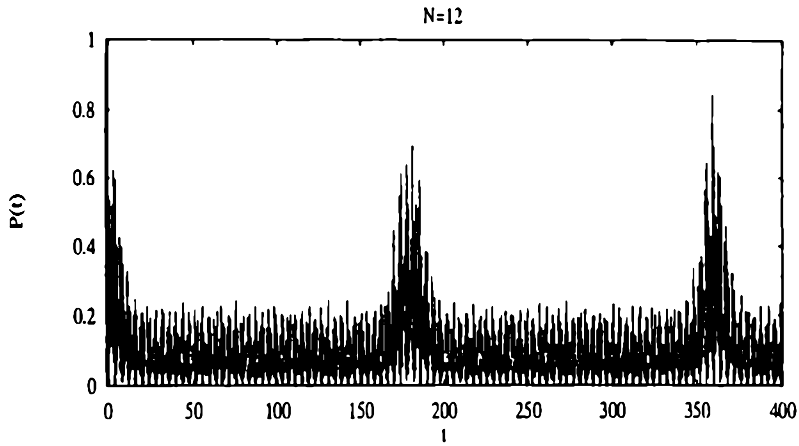

Fig. 7. Hypothetical recurrence probability for the electronic wave packet, excited to $\overline{n} = 12$, in uranium ion. Spin–orbit term included in the first order perturbation theory. Time units as in Fig. 4

Hipotetyczne prawdopodobieństwo powtórzenia dla pakietu falowego reprezentującego elektron, wzbudzonego do $\overline{n} = 12$; w jonie uranu. Człon spin–orbita włączony w pierwszym rzędzie rachunku zaburzeń. Jednostki czasu, jak na rycinie 4

$T_{\rm clas}$ of the order of tens picoseconds. As this time scales as $\overline{n}^3/Z^2$ coming to the considered uranium ion system one arrives with $T_{\rm clas}$ of the order 10^6 shorter (laser frequencies in the range of THz instead of MHz). This is already a range of X–ray lasers (which needs to be tunable for making experiments with wave packets).

Another idea that needs to be worked out is connected with stationary wave packets, quite recently discovered [14–17]. These packets are stabilized by an appropriate, circularly polarized electromagnetic field and in principle live forever. Then T_{ls} need not be so small and one can come back to systems with $Z = 1$ and high quantum numbers. The presence of additional electromagnetic field besides the Coulomb one makes, however, additional computational complications for attempts to include the spin–orbit interaction into considerations.

PACS numbers: 03.65.Sq;03.65.Ge;32.90+a.

REFERENCES

[1] Parker J., Stroud C. R., Jr., *Phys. Rev. Lett.*, 56 (1986) 716.

[2] Wals J., Fielding H. H. and van Linden van den Heuvell H. B., *Physica Scripta, T* 58 (1995) 62.
[3] Averbukh I. S., Perelman N. F., *Phys. Lett., A* 139 (1989) 449.
[4] Dačić-Gaeta Z., Stroud C. R. Jr., *Phys. Rev., A* 42 (1990) 6803.
[5] Peres A., *Phys. Rev., A* 47 (1993) 5196.
[6] Arvieu R., Rozmej P. *Phys. Rev., A* 50 (1994) 4376.
[7] Arvieu R., Rozmej P. *Phys. Rev., A* 51 (1995) 104.
[8] Rozmej P., Arvieu R., *J. Phys., B* 29 (1996) 1339.
[9] Rozmej P., Arvieu R., *Acta Phys. Polon.*, 27 (1996) 581.
[10] Rozmej P., Arvieu R., *Proc. Int. Conf. Nonlinear Dynamics, Chaotic and Complex Systems*, Zakopane, Poland, 7-12 November, 1995.
[11] Blum R., Kostelecky V. A., *Phys. Lett., A* 200 (1995) 308.
[12] Percival I. C., *J. Math. Phys.*, 2 (1961) 235.
[13] Borneis S. et al., *GSI Scientific Report*, 1 (1994) 152.
[14] Bialynicki-Birula I., Kalinski M. and Eberly J. H., *Phys. Rev. Lett.*, 73 (1994) 1777.
[15] Kalinski M., Eberly J. H. and Bialynicki-Birula I., *Phys. Rev. A*, 52 (1995) 2460.
[16] Buchleitner A., Delande D., *Phys. Rev. Lett.*, 75 (1995) 1487.
[17] Delande D., Zakrzewski J. and Buchleitner A., *Europhys. Lett.* 32 (1995) 107.

STRESZCZENIE

Przedmiotem naszych badań jest kwantowa dynamika paczek falowych w potencjale oscylatora harmonicznego oraz w atomach wodoropodobnych. Szczególną uwagę zwracamy na przypadki o małej średniej wartości głównej liczby kwantowej, ponieważ w takich warunkach istnieją szanse na wykrycie nowych struktur kollapsu i odbudowy pakietów, spowodowanych oddziaływaniem spin-orbita, w doświadczeniu. Uniwersalny scenariusz ciągu kollapsów, a także częściowej i całkowitej odbudowy pakietów znany w granicy dużych liczb kwantowych nie daje się bezpośrednio przenieść na małe liczby kwantowe. Istnienie bardzo dobrze odbudowanych pakietów w długiej ewolucji czasowej, wykazane tu numerycznie, sugeruje możliwość obserwacji częstości wahadła spinowo-orbitalnego i odróżnienia ich od częstości związanych ze standardowym kollapsem i odbudową pakietu, w odpowiednio przygotowanych eksperymentach.